THE JOURNAL OF PHYSICAL CHEMISTRY Letters

Letter

pubs.acs.org/JPCL

High Open-Circuit Voltage Solar Cells Based on Organic–Inorganic Lead Bromide Perovskite

Eran Edri,[†] Saar Kirmayer,[†] David Cahen,* and Gary Hodes*

Department of Materials and Interfaces, Weizmann Institute of Science, Rehovot, 76100, Israel

ABSTRACT: Mesoscopic solar cells, based on solution-processed organic–inorganic perovskite absorbers, are a promising avenue for converting solar to electrical energy. We used solution-processed organic–inorganic lead halide perovskite absorbers, in conjunction with organic hole conductors, to form high voltage solar cells. There is a dire need for low-cost cells of this type, to drive electrochemical reactions or as the high photon energy cell in a system with spectral splitting. These perovskite materials, although spin-coated from solution, form highly crystalline materials. Their simple synthesis, along with high chemical versatility, allows tuning their electronic and optical properties. By judicious selection of the perovskite lead halide-based absorber, matching organic hole conductor, and contacts, a cell with a ∼ 1.3 V open circuit voltage was made. While further study is needed, this achievement provides a general guideline for additional improvement of cell performance.

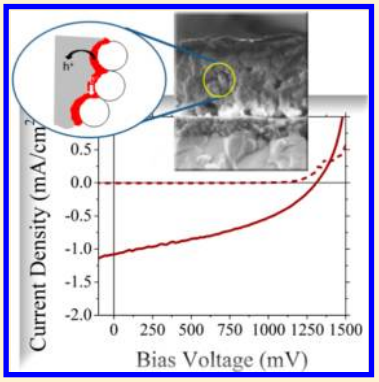

SECTION: Energy Conversion and Storage; Energy and Charge Transport

High open-circuit voltage solar cells are an important tool in the efforts for solar energy harvesting, both to drive electrochemical reactions,[1] and to function as a high-energy photon absorber in a system with spectral splitting to improve utilization of the solar spectrum.[2] To achieve a high open-circuit voltage in a solar cell, it is necessary to combine a suitable energy band structure of the constituent materials with good charge transfer kinetics. Organic–inorganic lead halide perovskites were introduced and studied, originally by Mitzi and co-workers,[3−6] mostly as the active layer in light-emitting diodes and field-effect transistors. The interest in these materials was driven mainly by their charge carrier mobilities, which are, at up to 50 cm^2/V-s, high for solution-processed materials. Another attractive aspect of this class of perovskites is the ability to tune their optical and electronic properties by changes in the chemical composition (changes in the alkyl group, metal atom and halide).[7−12] Recently, such perovskite materials were shown to be promising light absorbers or hole conductors in solar cells.[13−17]

Methylammonium lead iodide and lead bromide absorbers were implemented as sensitizers for titania in a liquid junction solar cell to give an open-circuit voltage of 0.61 V and efficiency of 3.8% for a $CH_3NH_3PbI_3$-based cell; a higher photovoltage of 0.96 V was obtained with a $CH_3NH_3PbBr_3$-based cell with 3.1% power conversion efficiency.[18] In similar work, after some optimization of the $CH_3NH_3PbI_3$-based cell, J_{SC} of 15.8 mA/cm^2, V_{OC} of 0.71 V, and fill factor of 0.59 were achieved, giving a 6.5% power conversion efficiency.[15] These cells demonstrated good charge separation kinetics. Recently, also good charge transport properties of the perovskites were demonstrated, as a 7.3% efficiency at 0.1 sun conditions was reported with $CH_3NH_3PbI_3$, on mesoporous titania,[16] where the perovskite is both the absorber as well as the hole conductor. When $CH_3NH_3PbI_3$ was used to sensitize titania in conjunction with spiro-OMETAD as the hole conductor, a 9.7% power conversion efficiency was achieved under 1 sun illumination.[14] The most remarkable result with these materials came when they were used in a different type of cell by switching from a sensitized to bulk heterojunction-like cell. Snaith and co-workers showed a top performance of 10.9% efficiency with a V_{OC} of 1.1 V, based on a $CH_3NH_3PbI_2Cl$ layer deposited on a mesoporous alumina scaffold and with spiro-OMETAD as the hole conductor.[13] This mesoscopic solar cell uses alumina that is presumed to be electronically inert as a scaffold for a several nanometer thick layer of perovskite, while the interdigitated spiro-OMETAD collects the holes and transfers them to the back electrode.

Here we show that by harnessing this novel type of organic–inorganic hybrid heterojunction-like structure, an avenue for high open-circuit voltage solar cells can be opened. The high charge carrier mobility of the perovskite, along with its relatively high dielectric constant and low-lying valence band, allows for the generation of high voltages. If tailored with the right hole conductor, having both a low-lying HOMO level as well as the appropriate electronic and optical properties, a solar cell with high open circuit voltage of up to 1.3 V is achieved.

The normalized transmission and emission spectra of the $CH_3NH_3PbBr_3$ film are given in Figure 1a. A Tauc plot [$(\alpha h\nu)^2$ vs $h\nu$ for a direct bandgap semiconductor – not shown] gives a bandgap of 2.32 eV. If excited with 375 nm light, the film exhibited a strong and relatively narrow emission peak centered at a slightly red-shifted position of 543 nm (2.29 eV).

Received: February 15, 2013
Accepted: February 28, 2013
Published: February 28, 2013

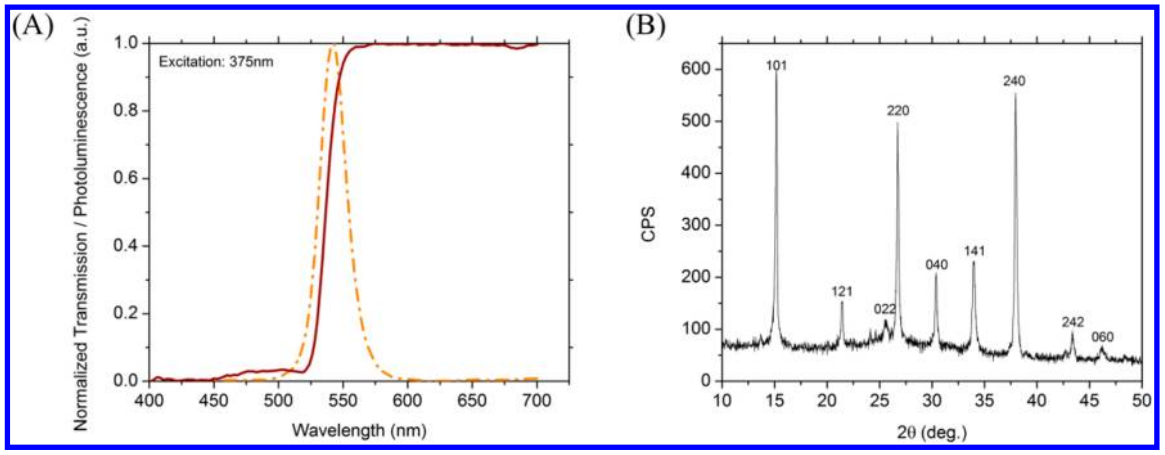

Figure 1. (A) Normalized transmission (solid line) and luminescence (dashed line) spectra of a $CH_3NH_3PbBr_3$ film on glass. The luminescence was measured with 375 nm excitation. (B) X-ray diffraction pattern of $CH_3NH_3PbBr_3$ deposited on mesoporous alumina film with indexing of the major peaks.

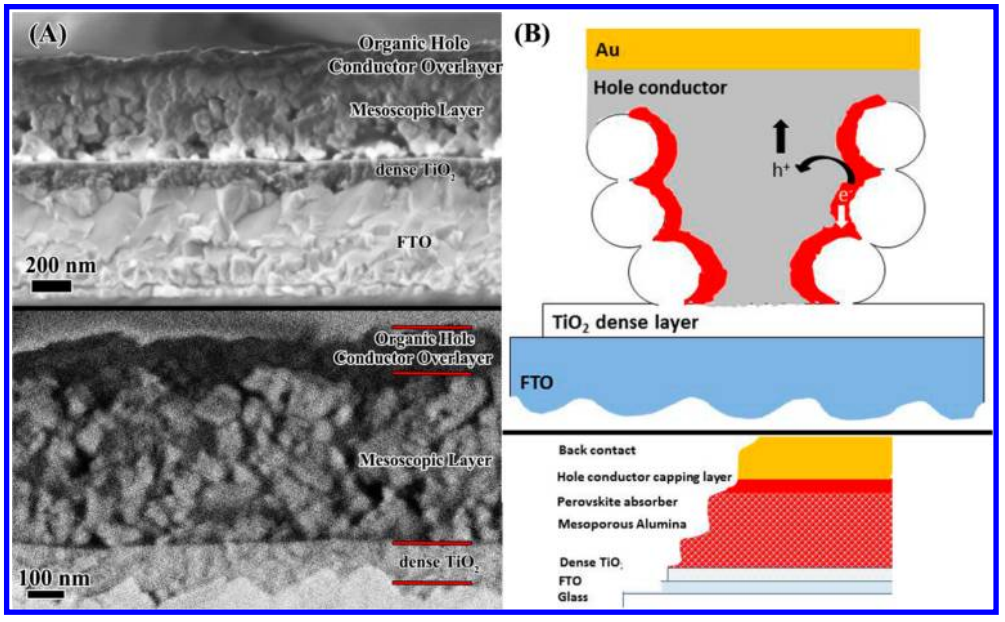

Figure 2. (A) SEM images of cross section of a solar cell: (top) image with in-lens detector; (bottom) image with backscattered electron detection, which is sensitive to the atomic number of the constituents, showing the distribution of lead through the layer and an overlayer of the organic hole conductor (note the different length scales of top and bottom images); (B) Schematics of cell with suggested operation principle on alumina substrate.

The X-ray diffraction pattern, taken from a film, spin-coated on a 500 nm mesoporous alumina substrate, given in Figure 1b, shows nine sharp reflections peaks at the following 2θ values: 15.2°, 21.4°, 25.6°, 26.7°, 30.4°, 33.9°, 34.4°, 37.9°, 43.4°, 46.0°, corresponding to the (1 0 1), (1 2 1), (0 2 2), (2 2 0), (0 4 0), (1 4 1), (2 4 0), (2 4 2), and (0 6 0) reflections of $CH_3NH_3PbBr_3$ (PDF#01-076-2758). Interestingly, although the measurement was done on crystals that were spin-coated on a mesoporous alumina substrate, many of the perovskite peaks did not appear in the diffraction pattern; this can be explained by preferred orientation in the (1 0 1) and (2 4 0) directions. In addition, it is important to note that the width of the diffraction peaks at the full width at half-maximum (fwhm) is close to the instrumental broadening limit (0.08°), indicating the formation of very large crystals inside the pores. It is currently unclear what the cause for such a growth pattern is, and further study is needed. As there is no sign of perovskite growth on top of the mesoporous layer, we postulate that the perovskite crystals grow in the pores that exist in the alumina, and that the preferred orientation observed by us and others explains the narrow width of the observed diffraction peaks.[19]

A secondary electron scanning electron microscopy (SEM) image of a mesoscopic solar cell cross section is shown at the top of Figure 2A. The image shows a device thickness of ca. 600 nm, consisting of a mesoporous layer with an organic overlayer, on top of a uniform dense titania layer. The backscattered electron image of the same cell, which is given on the bottom of Figure 2A, allows us to see the uniform distribution of the perovskite absorber throughout the cell cross section, shown as brighter spots, due to the high Z (atomic number) of the Pb in the absorber. In addition, the overlayer of the organic conductor (darker layer on top) is seen to uniformly cap the mesoporous layer. On top of this organic conductor is seen the top gold contact (the brighter thin layer in the two images). The cell schematic is given in Figure 2B.

dx.doi.org/10.1021/jz400348q | J. Phys. Chem. Lett. 2013, 4, 897−902

Table 1. Materials Properties

	Hole Mobility (cm^2/V·sec)	HOMO level (eV)	Absorption edge (nm) (*eV*)	ref.
P3HT	<0.1	−5.1	635 (*1.95*)	23
TPD	[a] 8.3×10^{-4}	−5.4	420 (*2.95*)	24
PDI	[a] 2.1	−5.8	540−600 (*2.30 − 2.05*)	25
PCBM	10^{-2}−10^{-3}	−6.1	520 (*2.40*)	26
$CH_3NH_3PbBr_3$	NA	−6.5 ± 0.2	540 (*2.30*)	from XPS

[a]Theoretical value.

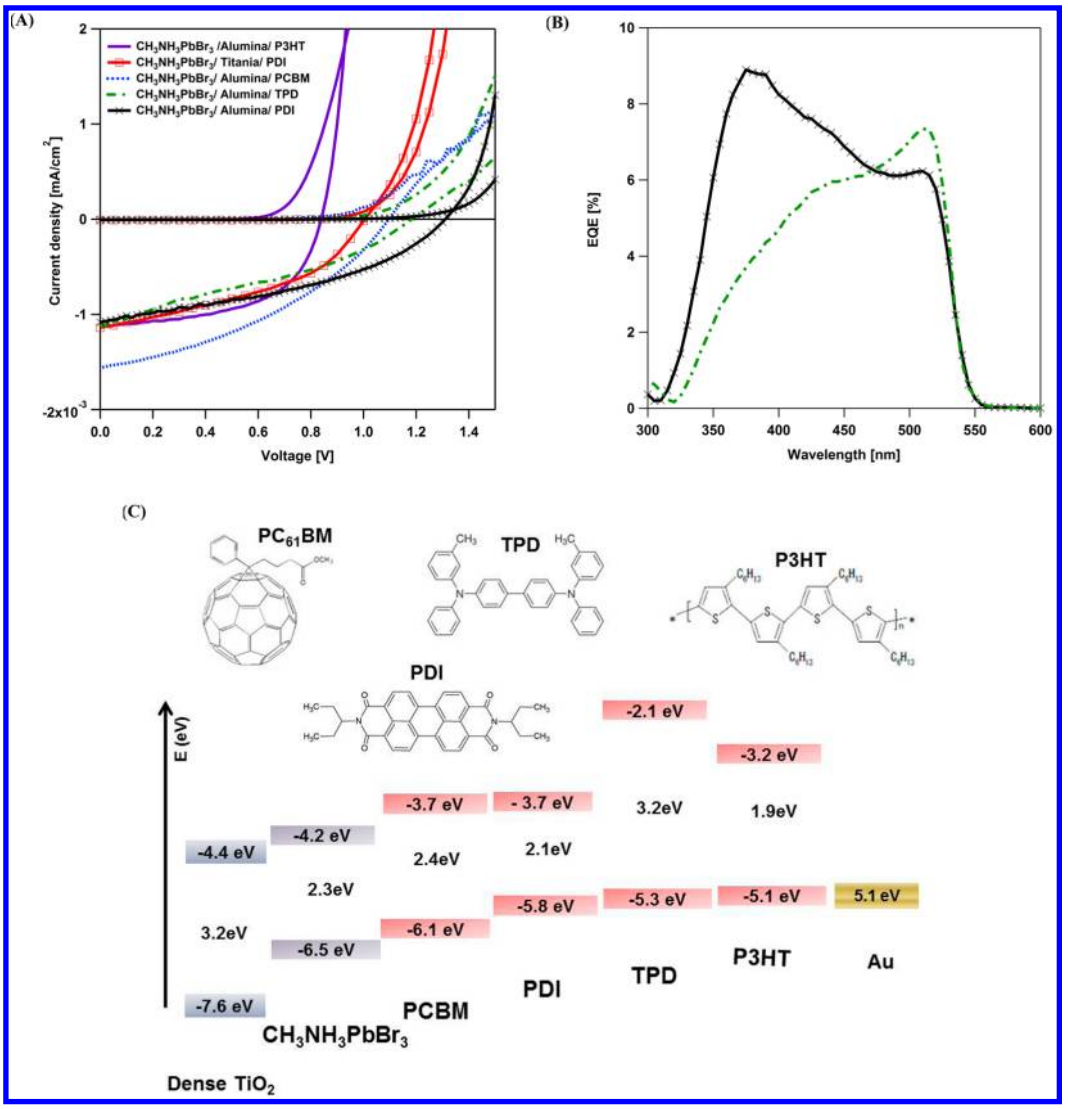

Figure 3. (A) Current density vs voltage curve of mesoscopic solar cells with $CH_3NH_3PbBr_3$ as absorber and various organic hole conductors: P3HT (purple solid line), TPD (green dash-dot line), PCBM (blue dotted line), and PDI (black solid lines with X), all on alumina scaffold. TiO_2-based cell with PDI is shown as well (red line with open square symbols). (B) External quantum efficiency of two examples: PDI and TPD as hole conductors on alumina. (C) Schematic of hole conductor chemical structure and energy level alignment of the different components. This schematic shows literature values for the frontier orbital energy levels of hole conductors, the conduction and valence band edges of the dense TiO_2, and the work function of Au; the values for the dense titania and perovskite are measured by us; it is very probable that at least some of these levels change with respect to each other, if brought into contact with each other. Alumina is not shown in this schematic, because it is supposed to be electronically inactive, and the band edges are expected to be outside the range spanned by the other band edges. Additionally, the band gaps and, even more important, band edge positions, reported in the literature are spread over a wide range.

Cells on two types of substrates are demonstrated. The first is based on mesoporous alumina, and the second is based on mesoporous TiO_2. These two types do not just differ in the type of oxide that forms the mesostructure, but the difference extends to the actual mechanism of photovoltaic action. In cells with the alumina as the scaffold, photogenerated electrons are not injected into the nanoporous oxide layer, but rather they flow through the perovskite absorber to the front electrode, while the holes are injected to the organic hole conductor and flow through it to the back contact. In the second type of cells, those with mesoporous TiO_2, a sensitizing mechanism is also possible, i.e., photogenerated electrons are injected into the

dx.doi.org/10.1021/jz400348q | J. Phys. Chem. Lett. 2013, 4, 897−902

TiO_2 and transported through it to the FTO electrode. Therefore, this latter type of cell acts as an extremely thin absorber cell (ETA).[20] We note that in both cell types, carriers need to pass through a dense TiO_2 layer to reach the transparent electrode, which presents a possible cause for voltage loss due to offsets between the perovskite and TiO_2 conduction bands. However, as pointed out in ref 13, for a flat dense layer, this voltage loss is expected to be much smaller than for a mesostructured TiO_2 layer. A common feature to both cell types is the short diffusion length for holes, which apparently is an important characteristic, as both cells without a hole conductor and those in a layered morphology ("flat cells") give poorer solar cells in terms of J_{SC} and V_{OC} (0.27 V, 0.8 mA/cm^2; results not shown).

Four types of organic materials were tested as hole conductors for these devices: poly-(3-hexyl)thiophene (P3HT), *N*,*N*′-dialkyl perylenediimide (PDI), *N*,*N*′-bis(3-methylphenyl)-*N*,*N*′-diphenylbenzidine (TPD), and [6,6]-phenyl-C_{61}-butyric acid methyl ester (PCBM). Their reported electronic properties are summarized in Table 1, and their schematic structure is given in Figure 3C along with the energies of the levels/bands that are relevant for the cell. We note that, while P3HT and TPD are usually used as *hole* carriers in organic electronic devices, PDI and PCBM are usually used as either *electron* acceptors or conductors. Each of these four materials was used as the hole conductor in solar cells with $CH_3NH_3PbBr_3$-coated alumina or titania scaffolds, and characterized under 1-sun illumination. The *J*−*V* curves and IPCE of typical hybrid device structures described earlier in Figure 2B are given in Figure 3, and the cell performance parameters are summarized in Table 2. If alumina was used as the scaffold, open circuit voltages of 840, 1100, 1200, and 1300 mV were achieved for P3HT, PCBM, TPD, and PDI, respectively, with short circuit currents of ca. 1.1−1.5 mA/cm^2. The open circuit voltage of these cells corresponds well with the reported highest occupied molecular orbital (HOMO) level energies of the organic hole conductors: V_{oc} increases as the energy of the HOMO level is reduced in relation to the vacuum level (see energy levels in Figure 3C). However, the J_{SC} of the cells is lower than expected from an absorber with 2.3 eV band gap (ca. 9 mA/cm^2),[21] and also the fill factors of the cells are low. The first is largely a result of low light absorption, because, at present, the films are optically too thin for complete absorption (the perovskite absorption in the cells is typically 30−50% - not shown). The second is most likely a result of high series resistance in the organic hole conductor. The thickness of the cell is a compromise between the need for good absorption of light and the thickness through which the hole conductor can penetrate and efficiently transfer holes to the back electrode. The cells with titania usually showed lower photovoltages than the alumina ones; however, a 1 V open circuit voltage was obtained for a TiO_2/ $CH_3NH_3PbBr_3$/PDI cell as shown for the best performing cells in Figure 3A (red line with open square symbols). If mesoporous titania is used, the photogenerated electrons can cover most of the distance to the electrode either in the perovskite or in this titania. In the latter case, electron injection occurs at an energy level, determined by the TiO_2 tail state density, i.e., well below the TiO_2 conduction band edge, and, therefore, the quasi Fermi-level splitting will be smaller than if electron flow is primarily in the perovskite layer.

Table 2. Cell Performance

device structure[b]	V_{OC}	J_{SC}	FF (%)	PCE (%)
alumina\$CH_3NH_3PbBr_3$\P3HT	0.84	1.13	54	0.52
alumina\$CH_3NH_3PbBr_3$\TPD	1.20	1.22	46	0.67
alumina\$CH_3NH_3PbBr_3$\PCBM	1.06	1.57	43	0.72
alumina\$CH_3NH_3PbBr_3$\PDI	1.30	1.08	40	0.56
titania\$CH_3NH_3PbBr_3$\PDI	1.00	1.14	41	0.47

[b]All devices were made on FTO with a compact layer of titania.

Since all of the hole conductors used in this work absorb light in the UV−vis range of the solar spectrum, which overlaps with the perovskite absorption, the question arises as to whether there is a contribution to the current generation not only from the perovskites, but also from the hole conductor. To check this, we measured the external quantum efficiency (EQE) of the cells. In Figure 3B we show results for TPD and PDI cells, which show lower EQE in spectral regions where the hole conductor absorbs, ∼400 nm for TPD and 540−600 nm for PDI. This indicates that that not only does the hole conductor not contribute photogenerated current, but that light absorbed in the hole conductor is lost in terms of power output from the cell. This might be overcome by using a hole conductor that absorbs only in the UV region, with similar, or better mobility, and a higher-lying HOMO level.[22]

At present, we surmise that the high open circuit voltage generation stems from the unique combination of properties of the lead bromide perovskites. The relatively low binding energy of the excitons[27] (compared with pure organic materials) and high charge mobility facilitates electron/hole separation and charge (in particular electron) transport to the electrodes. The low work function, measured at ca. −5.0 eV, in combination with the valence band energy level (ca. −6.5 eV), allows a nearly 800 mV light-induced shift (toward the conduction band) for the quasi-Fermi level of the perovskite. The high crystallinity of the perovskite furthermore minimizes band tailing, further increasing the maximum open-circuit voltage that can be achieved.[28] The rest of the measured open circuit voltage probably contributed by the shift of the quasi-Fermi level in the organic hole conductor. The lower the HOMO level of the hole conductor, the larger the difference between the quasi-Fermi levels can be, and the higher the photovoltage, as seen in the results. It is important to note that both the perovskites as well as the organic materials are capable of ambipolar conduction. However, in all these cells, holes are prevented from exiting through the front contact by the presence of the hole-blocking dense titania layer, which serves as a selective contact.

To conclude, we have shown that solar cells with high open circuit voltages can be made, based on mixed organic halide perovskite absorbers/electron conductors and organic semiconductor films with low HOMO levels, and that this is possible in both of the photovoltaic modes that Snaith et al.[13] showed to be possible with these perovskites, i.e., as a bulk heterojunction cell and as an ETA cell. It is not yet clear from these results whether the cell acts as a bulk heterojunction cell with a scaffold to support high surface area and a small diffusion length for the minority carriers, or whether there is an electric field that aids charge separation. At the moment, we can identify a few limiting factors to focus on to increase the current, fill factor, and open circuit voltage. Light absorption in these cells is not complete, but electrode thickness is limited by the hole conductor and/or the perovskite infiltration, forming a percolating self-connected network that will allow better charge

dx.doi.org/10.1021/jz400348q | J. Phys. Chem. Lett. 2013, 4, 897−902

transport. Second, the energy required to split the photogenerated charges in the perovskite hybrid solar cell, energy that is supplied by the offset in lowest unoccupied molecular orbital (LUMO) levels of the donor/absorber and acceptor in organic molecule/polymer-based cells, is smaller in these solar cells due to the higher dielectric constants of the perovskites, and, therefore, a lower exciton binding energy than obtained in all-organic cells. Therefore, there is still voltage to be gained by using a hole conductor with a lower lying HOMO level, although it is advisable to go this road only after higher currents have been realized. Third, in order to maximize the V_{OC}, one needs to use contacts with a large difference in work functions, preferably ones that match the work function of the electron and hole conductors, while here, contacts with similar work functions were used. With more optimal work function values, both a further increase in V_{OC} and improved charge separation should be possible.

EXPERIMENTAL METHODS

F-doped tin oxide (FTO) transparent conducting substrates were cut and cleaned by sequential 30 min sonication in acetone, ethanol, warm aqueous alconox solution, and deionized water, followed by drying in a N_2 stream. For the sol−gel solution, 2.7 mL of titanium(IV) isopropoxide (Sigma-Aldrich) was added to 71 mL of isopropanol and 1.0 g of diethanolamine (Fluka); after mixing for 5 min at room temperature, 70 μL of deionized water were added, and the sol was left to age for an hour. The sol-solution was spin-coated on the clean substrates at 4000 rpm for 25 s, followed by annealing. TiO_2 annealing was done in air, by ramping slowly (5 °C/min) to 160 °C, with a dwell time of 1 h at that temperature and then raising the temperature to 450 °C with a dwell time at that temperature for another hour. This process was carried out a total of 5 times to produce a flat, dense titania layer.

An alumina paste was made by dispersing the alumina (50 nm particle size) in ethanol and mixing with 3.33 gr α-terpineol for every 1 g of Al_2O_3, 1 g of 10 cP ethyl cellulose, and 1 g of 46 cP ethyl cellulose. A mesoporous Al_2O_3 scaffold was prepared by spin-coating (500 rpm for 5 s followed by 3000 rpm for 45 s) this paste followed by sintering at 550 °C for 30 min. Mesoporous titania was prepared by spin coating a 25 nm suspension containing 0.2 g of P25 (a gift from Evonik) in 5 mL ethanol, and 1 mL of 20 mg/mL polyethylene glycol (8K, Fluka) dissolved in acetonitrile, at 3000 rpm for 25 s, followed by annealing under the same conditions as those given above for the dense TiO_2.

A $CH_3NH_3PbBr_3$ solution was prepared as described elsewhere.[18] In short, CH_3NH_3Br was prepared by mixing methyl amine (40% in methanol) with hydrobromic acid (48% in water; CAUTION: exothermic reaction) in a 1:1 mol ratio in a 100 mL flask under continuous stirring at 0 °C for 2 h. CH_3NH_3Br was then crystallized by removing the solvent in an evaporator, washing three times in diethyl ether for 30 min, and filtering the precipitate. The material, in the form of white crystals, was then dried in vacuum at 60 °C for 24 h,. It was then kept in a dark, dry environment until further use. A 20 wt % solution of $CH_3NH_3PbBr_3$ was prepared by mixing $PbBr_2$ and CH_3NH_3Br in a 1:1 molar ratio in *N*′*N*-dimethylformamide (DMF). To coat the mesoporous substrate, the solution was spread on the surface and allowed to stand for 1 min before spinning at 1000 rpm for 20 s. The substrate was then heated on a hot plate set at 100 °C for 45 min. An orange-yellow color appeared on the surface.

Twenty milligram per milliliter solutions of P3HT (Rieke Metals), PDI, TPD (Sigma-Aldrich), and PCBM, were prepared by dissolving the materials in dichlorobenzene or chlorobenzene. Anhydrous solvents were used unless stated otherwise. The materials were spin-coated on the perovskite-coated mesoporous substrate at 1500 rpm for 45 s. One hundred nanometer gold contacts were thermally evaporated on the back through a shadow mask with 0.03 cm^2 holes.

The *I*−*V* characteristics were measured with a Keithley 2400-LV SourceMeter and controlled with a Labview-based, in-house designed program. A solar simulator (ScienceTech SF-150) calibrated with a Si solar cell IXOLAR High Efficiency SolarBIT (IXYS XOB17-04x3) was used for illumination.

X-ray diffraction (XRD) was done in the θ−2 θ configuration with a Rigaku ULTIMA III diffractometer, using Cu Kα radiation (at 40 kV and 40 mA) with 0.02° resolution. X-ray photoemission spectroscopy (XPS) was carried out on a Kratos AXIS ULTRA-DLD system, using a monochromatic Al (Kα) X-ray source (hν = 1486.6 eV) at 75 W and detection pass energies between 10 and 80 eV.

SEM images were taken on a Zeiss ULTRA or SUPRA high-resolution microscope. No special preparation procedures were taken, except with the cross-section images, where the sample was cleaved, just before putting it into the high vacuum chamber.

AUTHOR INFORMATION

Author Contributions

[†]These authors have contributed equally to this work.

Notes

The authors declare no competing financial interest.

ACKNOWLEDGMENTS

We wish to thank Dr. Hagai Cohen for the XPS measurements, and Dr. Boris Rybtchinski and Yaron Tidhar for providing the perylene diimide. We are grateful to the Israel Ministry of Trade and Industry via its KAMIN program, the Israel Ministry of Science and Technology, the Wolfson Family trust, the Leona M. and Harry B. Helmsley Charitable Trust, and the Nancy and Stephen Grand Center for Sensors and Security for partial support. D.C. holds the Sylvia and Rowland Schaefer Chair in Energy research.

REFERENCES

(1) Bard, A. J.; Fox, M. A. Artificial Photosynthesis - Solar Splitting of Water to Hydrogen and Oxygen. *Acc. Chem. Res.* **1995**, *28*, 141−145.
(2) Sven, R.; Akiba, S.; Ayelet, V.; Sarah, R. K.; Larissa, G.; Arie, Z.; Igor, L.; David, C. A Two Junction, Four Terminal Photovoltaic Device for Enhanced Light to Electric Power Conversion Using a Low-Cost Dichroic Mirror. *J. Renewable Sustainable Energy* **2009**, *1*, 013106.
(3) Mitzi, D. B. Solution-Processed Inorganic Semiconductors. *J. Mater. Chem.* **2004**, *14*, 2355−2365.
(4) Mitzi, D. B.; Chondroudis, K.; Kagan, C. R. Organic-inorganic electronics. *IBM J. Res. Dev.* **2001**, *45*, 29−45.
(5) Mitzi, D. B.; Feild, C. A.; Harrison, W. T. A.; Guloy, A. M. Conducting Tin Halides with a Layered Organic-Based Perovskite Structure. *Nature* **1994**, *369*, 467−469.
(6) Mitzi, D. B.; Wang, S.; Feild, C. A.; Chess, C. A.; Guloy, A. M. Conducting Layered Organic-Inorganic Halides Containing (110)-Oriented Perovskites Sheets. *Science* **1995**, *267*, 1473−1476.

(7) Kojima, A.; Ikegami, M.; Teshima, K.; Miyasaka, T. Highly Luminescent Lead Bromide Perovskite Nanoparticles Synthesized with Porous Alumina Media. *Chem. Lett.* **2012**, *41*, 397−399.
(8) Mitzi, D. B. Organic−Inorganic Perovskites Containing Trivalent Metal Halide Layers: The Templating Influence of the Organic Cation Layer. *Inorg. Chem.* **2000**, *39*, 6107−6113.
(9) Mitzi, D. B. Templating and Structural Engineering in Organic−Inorganic Perovskites. *Dalton Trans.* **2001**, 1−12.
(10) Mitzi, D. B.; Dimitrakopoulos, C. D.; Kosbar, L. L. Structurally Tailored Organic−Inorganic Perovskites: Optical Properties and Solution-Processed Channel Materials for Thin-Film Transistors. *Chem. Mater.* **2001**, *13*, 3728−3740.
(11) Knutson, J. L.; Martin, J. D.; Mitzi, D. B. Tuning the Band Gap in Hybrid Tin Iodide Perovskite Semiconductors Using Structural Templating. *Inorg. Chem.* **2005**, *44*, 4699−4705.
(12) Mitzi, D. B. Synthesis, Structure, and Properties of Organic−Inorganic Perovskites and Related Materials. In *Prog. Inorg. Chem.*; John Wiley & Sons, Inc.: New York, 2007; pp 1−121.
(13) Lee, M. M.; Teuscher, J.; Miyasaka, T.; Murakami, T. N.; Snaith, H. J. Efficient Hybrid Solar Cells Based on Meso-superstructured Organometal Halide Perovskites. *Science* **2012**, *338*, 643−647.
(14) Kim, H. S.; Lee, C. R.; Im, J. H.; Lee, K. B.; Moehl, T.; Marchioro, A.; Moon, S. J.; Humphry-Baker, R.; Yum, J. H.; Moser, J. E.; et al.. Lead Iodide Perovskite Sensitized All-Solid-State Submicron Thin Film Mesoscopic Solar Cell with Efficiency Exceeding 9%. *Sci. Rep.* **2012**, *2*.
(15) Im, J. H.; Lee, C. R.; Lee, J. W.; Park, S. W.; Park, N. G. 6.5% Efficient Perovskite Quantum-Dot-Sensitized Solar Cell. *Nanoscale* **2011**, *3*, 4088−4093.
(16) Etgar, L.; Gao, P.; Xue, Z. S.; Peng, Q.; Chandiran, A. K.; Liu, B.; Nazeeruddin, M. K.; Gratzel, M. Mesoscopic CH3NH3PbI3/TiO_2 Heterojunction Solar Cells. *J. Am. Chem. Soc.* **2012**, *134*, 17396−17399.
(17) Chung, I.; Lee, B.; He, J. Q.; Chang, R. P. H.; Kanatzidis, M. G. All-Solid-State Dye-Sensitized Solar Cells with High Efficiency. *Nature* **2012**, *485*, 486−494.
(18) Kojima, A.; Teshima, K.; Shirai, Y.; Miyasaka, T. Organometal Halide Perovskites as Visible-Light Sensitizers for Photovoltaic Cells. *J. Am. Chem. Soc.* **2009**, *131*, 6050−6051.
(19) The Scherrer equation holds for relatively isotropic particles only. For anisotropic particles that form anisotropic films, e.g., with oriented 1D or 2D growth as we assume we have here, the particle size in the direction of growth (and long-range order) will be concomitantly large. Here the order, in the direction of preferred growth, is such that we do not see any crystallite-related broadening, as the instrumental broadening dominates.
(20) Hodes, G.; Cahen, D. All-Solid-State, Semiconductor-Sensitized Nanoporous Solar Cells. *Acc. Chem. Res.* **2012**, *45*, 705−713.
(21) Bundgaard, E.; Krebs, F. C. Low Band Gap Polymers for Organic Photovoltaics. *Sol. Energy Mater. Sol. Cells* **2007**, *91*, 954−985.
(22) We also note that higher current densities are obtained under one sun illumination than the efficiencies in the EQE would suggest. There are several reasons that can explain this, such as white light/UV bias dependence and probe light intensity dependence.
(23) McCulloch, I.; Heeney, M.; Bailey, C.; Genevicius, K.; MacDonald, I.; Shkunov, M.; Sparrowe, D.; Tierney, S.; Wagner, R.; Zhang, W. M.; et al. Liquid-Crystalline Semiconducting Polymers with High Charge-Carrier Mobility. *Nat. Mater.* **2006**, *5*, 328−333.
(24) Kuwahara, A.; Naka, S.; Okada, H.; Onnagawa, H. Carrier Mobility of Organic Thin Films Using Lateral Electrode Structure with Optical Slits. *Appl. Phys. Lett.* **2006**, *89*.
(25) Delgado, M. C. R.; Kim, E. G.; Da Silva, D. A.; Bredas, J. L. Tuning the Charge-Transport Parameters of Perylene Diimide Single Crystals via End and/or Core Functionalization: A Density Functional Theory Investigation. *J. Am. Chem. Soc.* **2010**, *132*, 3375−3387.
(26) Tuladhar, S. M.; Poplavskyy, D.; Choulis, S. A.; Durrant, J. R.; Bradley, D. D. C.; Nelson, J. Ambipolar Charge Transport in Films of Methanofullerene and Poly(phenylenevinylene)/Methanofullerene Blends. *Adv. Funct. Mater.* **2005**, *15*, 1171−1182.
(27) Tanaka, K.; Takahashi, T.; Ban, T.; Kondo, T.; Uchida, K.; Miura, N. Comparative Study on the Excitons in Lead-Halide-Based Perovskite-Type Crystals $CH_3NH_3PbBr_3$ $CH_3NH_3PbI_3$. *Solid State Commun.* **2003**, *127*, 619−623.
(28) Nayak, P. K.; Garcia-Belmonte, G.; Kahn, A.; Bisquert, J.; Cahen, D. Photovoltaic Efficiency Limits and Material Disorder. *Energy Environ. Sci.* **2012**, *5*, 6022−6039.